AD_____

Award Number: DAMD17-02-1-0675

TITLE: Preparative Production of Acetylcholinesterase and Paraoxonase in Procaryotic and Eucaryotic Expression in Systems

PRINCIPAL INVESTIGATOR: J. L. Sussman, Ph.D.
I. Silman, Ph.D.

CONTRACTING ORGANIZATION: Weizmann Institute of Science
Rehovot 76100, Israel

REPORT DATE: January 2006

TYPE OF REPORT: Final

PREPARED FOR: U.S. Army Medical Research and Materiel Command
Fort Detrick, Maryland 21702-5012

DISTRIBUTION STATEMENT: Approved for Public Release;
Distribution Unlimited

The views, opinions and/or findings contained in this report are those of the author(s) and should not be construed as an official Department of the Army position, policy or decision unless so designated by other documentation.

REPORT DOCUMENTATION PAGE

Form Approved
OMB No. 0704-0188

Public reporting burden for this collection of information is estimated to average 1 hour per response, including the time for reviewing instructions, searching existing data sources, gathering and maintaining the data needed, and completing and reviewing this collection of information. Send comments regarding this burden estimate or any other aspect of this collection of information, including suggestions for reducing this burden to Department of Defense, Washington Headquarters Services, Directorate for Information Operations and Reports (0704-0188), 1215 Jefferson Davis Highway, Suite 1204, Arlington, VA 22202-4302. Respondents should be aware that notwithstanding any other provision of law, no person shall be subject to any penalty for failing to comply with a collection of information if it does not display a currently valid OMB control number. **PLEASE DO NOT RETURN YOUR FORM TO THE ABOVE ADDRESS.**

1. REPORT DATE *(DD-MM-YYYY)*	**2. REPORT TYPE**	**3. DATES COVERED** *(From - To)*
January 2006	Final	1 Jul 02 – 31 Dec 05

4. TITLE AND SUBTITLE
Preparative Production of Acetylcholinesterase and Paraoxonase in Procaryotic and Eucaryotic Expression in Systems

5a. CONTRACT NUMBER

5b. GRANT NUMBER
DAMD17-02-1-0675

5c. PROGRAM ELEMENT NUMBER

6. AUTHOR(S)
J. L. Sussman, Ph.D.
I. Silman, Ph.D.

E-Mail: Joel.Sussman@weizmann.ac.il

5d. PROJECT NUMBER

5e. TASK NUMBER

5f. WORK UNIT NUMBER

7. PERFORMING ORGANIZATION NAME(S) AND ADDRESS(ES)
Weizmann Institute of Science
Rehovot 76100 ISRAEL

8. PERFORMING ORGANIZATION REPORT NUMBER

9. SPONSORING / MONITORING AGENCY NAME(S) AND ADDRESS(ES)
U.S. Army Medical Research and Materiel Command
Fort Detrick, Maryland 21702-5012

10. SPONSOR/MONITOR'S ACRONYM(S)

11. SPONSOR/MONITOR'S REPORT NUMBER(S)

12. DISTRIBUTION / AVAILABILITY STATEMENT
Approved for Public Release; Distribution Unlimited

13. SUPPLEMENTARY NOTES

14. ABSTRACT

Members of the serum paraoxonase (PON) family have been identified in mammals and other vertebrates, and in invertebrates. PONs exhibit a wide range of physiologically important hydrolytic activities, including drug metabolism and detoxification of nerve agents. PON1 and PON3 reside on high-density lipoprotein (HDL, 'good cholesterol') and are involved in the prevention of atherosclerosis. We describe the first crystal structure of a PON family member, a variant of PON1 obtained by directed evolution, at a resolution of 2.2 A. PON1 is a six-bladed beta-propeller with a unique active site lid that is also involved in HDL binding. The three-dimensional structure and directed evolution studies permit a detailed description of PON1's active site and catalytic mechanism, which are reminiscent of secreted phospholipase A2, and of the routes by which PON family members diverged toward different substrate and reaction selectivities.

15. SUBJECT TERMS
X-ray crystallography, directed evolution, organophosphates, bioscavengers, HDL, beta-propeller

16. SECURITY CLASSIFICATION OF:			**17. LIMITATION OF ABSTRACT**	**18. NUMBER OF PAGES**	**19a. NAME OF RESPONSIBLE PERSON**
a. REPORT	**b. ABSTRACT**	**c. THIS PAGE**			USAMRMC
U	U	U	UU	38	**19b. TELEPHONE NUMBER** *(include area code)*

Table of Contents

Introduction

Serum paraoxonase (PON1) is a mammalian enzyme that catalyzes the hydrolysis and, thereby, inactivation of various organophosphates (OPs), including the nerve agents sarin and soman[1]. In recent years it has become apparent that PON1 plays important roles in drug metabolism and in prevention of atherosclerosis[1,2]. PON1 is the best-studied member of a family of mammalian enzymes that includes PON2 and PON3, which share ~60% sequence identity with PON1. PON1 and PON3 reside in the cholesterol-carrying HDL ("good cholesterol") particles, whereas PON2 is found in many tissues. Polymorphism of the PON1 gene affects the blood levels of PON1 and its catalytic efficacy; both factors have a major impact on the susceptibility to atherosclerosis, and to pollutants and insecticides[1]. Knockout mice lacking the PON1 gene are highly susceptible to atherosclerosis and to OP poisoning[3]. *In vitro* assays show that PON1 and PON3 inhibit lipid oxidation in LDL ("bad cholesterol"), thus reducing levels of oxidized lipids involved in the initiation of atherosclerosis[4,5]. Since atherosclerosis is the underlying cause of 50% of mortality in Western societies, and OPs comprise an environmental risk as well as a terrorist threat, PONs have recently become the subject of intensive research.

Despite many efforts, the structure and mechanism of action of PONs had remained enigmatic. The name, paraoxonase, is purely historical, since the PON family is a hydrolase family with one of the broadest specificities known. PON1 displays proficient esterase activity on several synthetic substrates, whilst PON2 and PON3 exhibit high lactonase activity. But the paraoxonase activity of PON1 is rather weak, and PON2 and PON3 exhibit almost no paraoxonase activity[1]. However, all these activities towards man-made chemicals are promiscuous activities of PONs rather than their primary function(s). A variety of physiological roles have been proposed for PONs, including phospholipase A2 action[6], degradation of oxidized lipids[7], and hydrolysis and inactivation of homocysteine thiolactone - a known risk factor for atherosclerotic vascular disease[8]. The anti-atherosclerotic activity of the PONs is intimately linked to their localization on HDL particles. It has been suggested that the hydrophobic N-terminus of PON1 mediates its anchoring to HDL[9].

Structural and functional characterization of the PONs, and their engineering, have been hindered by lack of an ample source of recombinant protein. We recently described the directed evolution of PON1 and PON3 variants that express in a soluble and active form in *E. coli*, and exhibit enzymatic properties identical to those reported for PONs purified from sera[10]. This enabled us to solve the crystal structure of a recombinant PON1 variant derived from rabbit PON1, which is highly similar to human PON1. By combining directed evolution, site-directed mutagenesis and kinetic studies, we have been able to provide a comprehensive description of the overall architecture of PON1, details of its active site, catalytic mechanism and HDL-binding mode. Our data show how directed evolution in the laboratory follows in the footsteps of natural evolution in swiftly providing new PON variants with pre-determined catalytic specializations.

Body

Crystallization and structure determination

Previous attempts to determine the structure of PON1 relied on limited amounts of serum-purified proteins, resulting in crystallization of a protein that co-purified with it[11]. Human PON1 is rather unstable, and tends to aggregate in the absence of detergents[12]. These factors led us to directly evolve PONs for bacterial expression and increased solubility[10]. Family shuffling of four PON1 genes (human, rabbit, mouse and rat), and screening for esterolytic activity, led to recombinant PON1 variants (rePON1s) that express in *E. coli*. These variants diverged from wild-type (wt) rabbit PON1 by 14-31 amino acids coming from other PON1 genes, and exhibit enzymatic properties essentially identical to those of wt PON1[10]. Variants from the 1st round of evolution aggregated, and none crystallized. The 2nd-generation variants (obtained by shuffling of the 1st generation variants and screening for highest expression levels) did not aggregate, and at least one (G2E6) gave stable and well diffracting crystals.

RePON1-G2E6 exhibits 91% sequence identity to wt rabbit PON1, with the majority of the variations deriving from human, mouse, or rat wt PON1. It should be noted that rabbit and human PON1s themselves are highly homologous in sequence (86%) and function[13]. Moreover, sequence variations between rePON1-G2E6 and rabbit and human PON1 are in regions that do not affect their active sites or overall structures. Both purified native rePON1-G2E6 and rePON1-G2E6 containing selenomethionine (SeMet-rePON1-G2E6) were crystallized, yielding isomorphous crystals of space group $P4_32_12$. The structure was solved by single isomorphous replacement anomalous scattering from data collected to 2.6Å on the SeMet crystals and to 2.2 Å on the crystals of the native protein[14]. The structure shows all residues except N-terminal residues 1-15 and a surface loop (72-79). Two calcium atoms, a phosphate ion, and 115 water molecules are also seen.

The overall architecture of PON1

PON1 is a 6-bladed β-propeller, with each blade containing 4 strands (Fig. 1). The 'velcro' closure characteristic of this fold[15] is supplemented by a disulphide bridge between Cys42 (strand 6D) and Cys353 (strand 6C). This covalent closure of the N- and C-termini is rarely seen in β-propellers with more than four blades, but is conserved throughout the PON family.

Two calcium ions, 7.4Å apart, are seen in the central tunnel of the propeller: one at the top (Ca-1) and one in the central section (Ca-2). Ca-2 is most probably a 'structural calcium' whose dissociation leads to irreversible denaturation[16]. Ca-1 is assigned as the 'catalytic calcium'[16]. It appears to interact with five protein residues (the side-chain oxygens of Asn224, Asn270, Asn168, Asp269 and Glu53), 2.2-2.5Å away. Two other potential ligands are a water molecule, and one of the oxygens of a phosphate ion. The two calcium ions exhibit markedly different affinities[13]. The ligation of Ca-1 is more extensive than that of Ca-2. However, two of Ca-1's ligating residues (Asn224, Asp269) exhibit distorted dihedral angles. This observation, together with the higher solvent accessibility of Ca-1, indicate that Ca-2 is the higher affinity calcium.

The 3D structure of PON1 resembles that of *Loligo Vulgaris* DFPase[17]. Both are 6-bladed propellers with two calcium atoms in their central tunnel. They also share functional homology, since both exhibit phosphotriesterase (PTE) activity, although PON1 is primarily an esterase or lactonase. However, there is no clear sequence homology between them (BLAST E-score >>3.6), although more sensitive algorithms indicate weak but significant similarity[11]. Closer inspection reveals that PON1 and DFPase differ significantly in their overall architecture, active-site structure and mechanism. In particular, PON1 possesses a unique addition in the form of an active-site canopy defined by helices H2 and H3 and the loops connecting them to the β-propeller scaffold. This addition provides PON with an uncharacteristically closed active site, since most β-propellers, including DFPase, exhibit uncovered active sites defined only by loops that connect the β-strands. It seems to play a critical role in PON1's function, both in defining the active-site architecture and sequestering it from solvent, and in anchoring PON1 to HDL.

Although detergent-solubilized PON1 forms dimers and higher oligomers[12], in the crystal there is only one molecule per asymmetric unit, and very few contacts between symmetry-related molecules. It is possible that crystallization favors a monomeric form, but it seems more likely that oligomerization of PON1 is a consequence of its anchoring to detergent micelles in a mode similar to its anchoring to HDL. Mammalian PON1 is glycosylated, but glycosylation is not essential for hydrolytic activity[10,18]. There are four potential *N*-glycosylation sites on PON1 (NX(S/T) sites). Two, Asn227 and Asn270, are in the central tunnel of the propeller, and are

largely inaccessible to solvent. Asn253 and Asn324 are located on surface loops, and are most probably, as previously proposed[18], PON1's glycosylation sites.

Directed evolution of substrate specificity

To understand better the role of promiscuity in natural evolution, we used laboratory-directed evolution, a tool that not only provides access to new tailor-made protein variants but also helps to refine our understanding of protein evolution[19].

Serum paraoxonase (PON1) was chosen as a target for evolution. We applied a process of random mutation and selection, with the aim of increasing its promiscuous activity. We applied only one selection pressure at a time (aiming to increase one promiscuous activity) and focused on the early evolutionary intermediates in which the first mutations that increased that promiscuous activity accumulated.

PON1 is the most studied member of a family of closely related enzymes that shares lactonase activity[1]. It efficiently catalyzes the hydrolysis and the formation of 5- and 6-member ring lactones[1]. PON1 also catalyzes the hydrolysis of a wide range of substrates that have no apparent physiological relevance, including aryl esters and organophosphates such as paraoxon.

We created genetic diversity in the gene encoding PON1 by error-prone PCR amplification under conditions that induced, on average, a few mutations per gene. The resulting gene libraries were cloned into an expression vector and used to transform *E. coli*. Several thousand clones from each of these libraries were plated on agar and screened with the target substrate. Positive colonies (as determined by the appearance of a colored or fluorescent product) were transferred to and grew in 96-well plates. The cells were then lysed, and the lysates assayed with the same substrate, using a spectrophotometric plate reader and comparing their activity to that of the wild-type enzyme. PON1 was allowed to evolve towards increased activity with four different promiscuous substrates. The catalytic efficiency of wild-type PON1 with these man-made, promiscuous substrates varied from very low to medium ($k_{cat}/K_M = 10^2–10^5\ M^{-1}s^{-1}$).

We isolated variants of each enzyme that had higher activity with the target substrate and shuffled them (*i.e.*, recombined them *in vitro*)[20] to yield second-generation gene libraries, which were then screened with the same substrate. Typically, we identified a few different mutations in individual first-round variants, which were combined by the *in vitro* recombination that followed the first and second rounds of screening. We focused our studies on the first steps after the recruitment of a promiscuous function and its improvement to provide a potential selective advantage.

The selected PON1 variants had substantial changes in activity (10–500 times higher than the wild-type enzyme) towards other promiscuous substrates that had not been selected for (Fig. 2). The substrate selectivities of these variants, relative to those of the wild-type enzyme, were as much as 3 x 10^4-fold higher. Thus, the selection pressure for improved activity led indirectly to 'specialization', although no selection pressure for specialization had been applied, since a decrease in activity towards substrates other than the target substrate was not applied as a selection criterion. In some cases, specialization completely reversed the selectivity towards the various promiscuous activities. For example, wild-type PON1 is an efficient aryl esterase ($k_{cat}/K_M \approx 2 \times 10^6$ $M^{-1}s^{-1}$ for phenyl acetate) with > 100 times weaker organophosphate hydrolase activity ($k_{cat}/K_M < 10^4$ $M^{-1}s^{-1}$ for organophosphates)[10], whereas the evolved variant 3.2PC has $k_{cat}/K_M \approx 10^6$ $M^{-1}s^{-1}$ for the organophosphate it was selected for and ~100 times lower esterase activity (Fig. 2). The most notable feature we observed in all the newly evolved variants was that the native activities changed comparatively little, in contrast to the promiscuous activities, which changed substantially.

It should be noted that the lactonase activity of the newly evolved PON1 variants barely changed (Fig. 2). Thus, all the evolutionary processes described above share the characteristic that mutations (few, or often a single one) that induce marked phenotypic changes in promiscuous activities have a much smaller effect (and sometimes no effect) on the native function. Conservation of the native function was not the result of a selection pressure: we applied only one selection criterion, an enhancement of one of the promiscuous activities..

The differential effect of mutations on native versus promiscuous functions is particularly notable in view of the fact that these mutations occur mostly in residues that form the walls and perimeter of the active site of PON1. The plasticity of these residues, and their potential contribution to the ability of proteins to evolve, is probably due to the fact that they are not part of the protein's scaffold, of other core elements of the fold, or of the actual catalytic machinery of the enzyme. They are on surface loops that are part of the substrate-binding pocket and display conformational flexibility (Fig. 3). A notable example of this principle is α-lytic protease, in which a single amino acid substitution increased the activity towards promiscuous substrates by a factor of 10^5 but reduced the native activity by only 2-fold[21]; the structural flexibility of the substrate-binding loops allowed this large shift in the selectivity of this enzyme and of its family members[21,22]. There may also be fundamental differences between the mode of binding of the native substrate, which is typically mediated by several independent, enthalpy-driven interactions, compared to that of the promiscuous substrates, in which hydrophobic and other entropy-driven interactions are important[23].

The catalytic mechanism

At the very bottom of the active-site cavity lie both the upper calcium (Ca-1) and a phosphate ion, which was present in the mother liquor (Fig. 4). One of the oxygens of this phosphate is only 2.2Å from Ca-1, and it may be bound in a mode similar to the intermediates in the hydrolytic reactions catalyzed by PON. One of its negatively charged oxygens, that nearest to Ca-1, may mimic the oxyanionic moiety of these intermediates stabilized by the positively-charged calcium. This type of 'oxyanion hole' is seen in secreted phospholipase A_2 (PLA_2)[24], and has also been suggested for DFPase[17]. Two other phosphate oxygens may be mimicking the attacking hydroxyl ion and the oxygen of the alkoxy or phenoxy leaving groups of ester and lactone substrates.

To help elucidate the mechanism of action of PON its pH-rate profile was determined with two typical substrates: an ester, 2-naphthyl acetate (2NA), and a phosphotriester, paraoxon. Both profiles exhibit a bell-shaped curve. The minor basic shoulder fits an apparent pK_a of 9.8 (paraoxon) or 9.0 (2NA), probably reflecting deprotonation of a basic side-chain that affects the active site but is not directly involved in catalysis. The fully pronounced acidic shoulder, of apparent pK_a ~7.1, may be ascribed to a His imidazole involved in a base-catalyzed, rate-

determining step. In hydrolytic enzymes, such an imidazole ring often serves as a base, deprotonating a water molecule and generating the attacking hydroxide ion that produces hydrolysis. In secreted PLA_2, the attacking hydroxide is generated by a His-Asp dyad, in which the imidazole acts as a base to deprotonate a water molecule, and the Asp carboxylate increases the imidazole's basicity via a proton-shuttle mechanism. The closest His nitrogen in PLA_2 is 6.3Å from the catalytic calcium, and two water molecules are involved: one attacking the substrate (after deprotonation), and another 'catalytic water' that mediates between the attacking water and the His base[24]. The DFPase active site also contains a His-Glu dyad with a His nitrogen 7.2Å from the catalytic calcium[17].

We asked ourselves whether PON1 adopted the same mechanism – namely a His-Glu/Asp dyad acting as base on a two-water-molecule cascade? PON1's active site contains such a dyad (Asp183, His184). However, His184 is ~11Å from Ca-1, and the His184Asn mutant of human PON1 is active[25]. Another putative dyad is His285-Asp269. Yet Asp269 ligates Ca-1, and His285 is ~8Å from Ca-1 and ~5Å from the nearest phosphate oxygen. We identified, however, a His-His dyad near both Ca-1 and the phosphate ion (Fig. 5). We hypothesized that His115 (the closer nitrogen of which is only 4.1Å from Ca-1) acts as a general base to deprotonate a *single* water molecule and generate the attacking hydroxide, while His134 acts in a proton shuttle mechanism to increase His115's basicity. Interestingly, His115 adopts distorted dihedral angles - a phenomenon observed in catalytic residues of many enzymes. This assignment for the catalytic mechanism was supported by the His115Gln mutation, which resulted in a dramatic decrease (~$2x10^4$ fold) in activity, and the His134Gln mutation, that produced a smaller, but substantial, decrease (6-150 fold).

However, following a recent report by Yeung and coworkers[26]who introduced the His115Trp mutation into human PON1, that is highly homologous to our recombinant PON1, we carried out further mechanistic studies. We thus discovered that our previous measurements of the His115Gln and His134Gln mutants were biased by two factors. First, the His115Gln mutant carried another mutation (His177Arg), which was accidentally incorporated during PCR amplification of the gene. In itself, this mutation of a residue far way from the active-site has little effect (paraoxonase and aryl-esterase activities are both ~70% of that of the parental PON1

gene). But the double His115Gln/His177Arg mutation led to an almost complete loss of activity.. Second, both mutants (His115Gln and His134Gln) are unstable and prone to loss of activity, misfolding, and ultimately aggregation. The same mutants (including the His115Gln mutant in isolation) were purified in the permanent presence of detergent (0.1% tergitol, incorporated into in the lysis, loading and elution buffers) and 10% glycerol, and assayed immediately after purification. Their activities are displayed in Table 2.

The existence (or even increase) in the paraoxonase activity of these mutants suggests that the new purification conditions, and the removal of the accidental His177Arg mutation, excluded the global effect of these mutations on protein stability and folding. Furthermore, we have since incorporated the same mutations into the recombinant PON1 variant G2E6, the one whose 3D structure was determined[14,27], and into another recombinant PON1 variant, G3C9, with similar results. Thus our most recent data suggest that His115 and His134 are not responsible for the paraoxonase activity of PON1, although they appear to significantly affect its aryl-esterase activity. Thus, the possibility must be considered that the two hydrolytic activities are catalyzed by different active-site residues, and that the His-dyad model postulated (Fig. 5) may be valid only for the aryl-esterase activity.

Cys284, which is conserved in all PONs, has been proposed to fulfill alternative functions of PON1 related to atherosclerosis[28]. It is part of a highly conserved stretch that includes active-site His285, and is packed against four highly-conserved residues from the adjacent strands (267, 268, 303 and 305; Fig. 6). Since it is buried, it is unlikely that it has a functional role. Its mutation, however, is likely to destabilize the core structure, thereby affecting function indirectly. Indeed, we found that Cys284 mutants of rePON1 are poorly expressed and relatively unstable.

Anchoring of PON1 to HDL

PON1 and PON3 are synthesized in the liver, and secreted into the blood, where they specifically associate with HDL. HDL is a particle of ~10 nm diameter, composed primarily of membrane components (phospholipids, cholesterol and cholesterol esters), and apolipoprotein A-

I (apoA-I)[29], the amphipathic helices of which are thought to wrap around the particle's membrane-like bilayer in a belt-wise manner[30].

PON1 retains its hydrophobic N-terminus, which resembles a signal peptide, and is thought to be involved in anchoring of PON1 to HDL[9]. Most of the N-terminus is disordered and invisible in the crystal structure; yet its hydrophilic part, which extends beyond the signal peptide (residues 19-28), adopts a helical structure (H1). The entire sequence of the N-terminus is compatible with a transmembrane helix; yet, following a secondary structure prediction, we modeled only residues 7-18 as part of H1 (Fig. 7). Helix H2, adjacent to H1, possesses a clearly amphipathic character. Unexpectedly, however, its hydrophobic face points towards the solvent, as do several residues from the two loops that connect H2 to the propeller scaffold. Helices H1 and H2 thus form two adjacent hydrophobic patches that clearly provide a potential membrane-binding surface (Fig. 7a). The interface with HDL is further defined by a characteristic 'aromatic belt' rich in Trp and Tyr side chains, and by a Lys side chain on H1[31]. Notably, the glycosylation sites point away from the interface (Fig. 7b).

The 3D-structure does provide a hint regarding the origins of PON1's remarkably wide substrate range. Hydrophobicity is common to almost all its effective substrates. The hydrophobicity and depth of PON1's active site explain this preference, and account for the fact that its substrates, whether poor or effective, exhibit K_M values in the millimolar range, but widely varying k_{cat} values[1,10]. PON1's multi-specificity is, therefore, driven primarily by non-specific hydrophobic forces, as observed for other enzymes that possess deep hydrophobic active sites, such as acetylcholinesterase[34]. We postulate that poor substrates, as well as effective ones, bind at the active site with similar affinity; yet the mode of binding differs, since the poor substrates are inadequately positioned relative to Ca-1 and to the catalytic base. It seems likely that the mutations observed following the directed evolution process reshape the walls and perimeter of the active site, thereby improving the positioning of some substrates (and of their respective catalytic intermediates and transition states) and worsening that of others. Reshaping of the active site walls is also the driving force behind the evolutionary divergence of various PON sub-families.

Polymorphism of the PON gene, and its effects on susceptibility to OP poisoning and to atherosclerosis, are the subject of intensive research. The two most common PON1 forms are Q/R192 and L/M55. The 3D structure of the recombinant PON crystallized reveals that Lys192 is part of the active-site wall. In human PON1, this position is normally arginine (R), but a commonly observed polymorphism to glutamine (192Q) results in an approximately 10-fold decrease in paraoxonase activity accompanied by a higher susceptibility to atherosclerosis[1]. Given the drastic effects of changes in other active-site residues on substrate selectivity (Table 3), the human 192Q variant may indeed exhibit significantly reduced activities towards PON1's physiological substrates, resulting in increased susceptibility to atherosclerosis. The L55M mutation may significantly affect PON1's stability, and thereby result in the lower enzymatic activity observed[35]. This may be ascribed to the key role of Leu55 in packing the propeller's central tunnel, and/or to the fact that its neighboring residues (Glu53 and Asp54) ligate both Ca-1 and Ca-2.

A detailed analysis of the amino acid variations between rePON1 variant G2E6 and wild-type Rabbit PON1

As mentioned above[10], all rePON1 variants that efficiently express in *E. coli* are chimeras of four mammalian PON1s (Human, Mouse, Rat and Rabbit) that show 79- 95% sequence identity by Clustal W analysis (Fig. 8). These PON1 genes were recombined to create the shuffled DNA library. The rePON1 variants were explicitly selected so that their enzymatic properties remain unchanged relative to wild type (wt) PON1. This functional identity was confirmed with over a dozen different substrates, including esters, phosphotriesters, lactones, thiolactones and esters of long-chain carboxylic acids. Their biological activities are also very similar to those of wt human and rabbit PON1. Selected variants were found to be most similar to RabPON1 (rabbit PON1) with fewer contributions from the other three parental wild type (wt) genes. Variant G2E6, for which the structure was solved, exhibits 91% similarity to RabPON1. Overall, there are 31 amino acid differences between rePON1-G2E6 and wt RabPON1. Twenty-eight of these differences come from other wt PON1 genes, and only three are mutations in the real sense. As analyzed below, these differences are all in regions that do not seem to affect the overall structure of the enzyme or its active site.

The amino acid differences between rePON1-G2E6 and wt RabPON1 can be divided into three groups (Table 4). The first group is comprised of 8 residues that originate from the other parental

genes (human, mouse and rat) and were found to be mostly within the interior of the protein (Fig. 9). These residues are conserved among all rePON1 variants that express efficiently in *E. coli* ([10] and Fig. 8). The structure indicates that several of these residues are in contact with each other. For example, Leu130 and Val143, that pack strand 2B against 2C, or Val320 (strand 5D), and Leu341 and Ile343 (strand 6B), that are critically located at the propeller's hydrophobic core between the fifth and the sixth blades. Residues of the first group most probably facilitate better packing of the hydrophobic core, and prevent misfolding and aggregation. Their absolute conservation amongst the rePON1 variants indicates that they are the key to soluble expression in *E. coli*. Their location, distant from the active site, explains why all the rePON1 variants exhibit enzymatic activity similar to that of wt PON1. The second group includes amino acids that are not conserved among other rePON1 variants (e.g. rePON1-G3C9), yet originate from the other parental PON1 genes (human, mouse and rat). These amino acids are located mostly on the protein surface (Fig. 9). Three of these residues (105, 107, 297) are involved in intermolecular contacts in the crystal. Hence they probably facilitate the successful crystallization of rePON1-G2E6. Most of the residues are far from the active site, at the bottom face of the propeller. Only one residue, Phe293, is part of PON1's active site. However, this residue anyway varies between Tyr (e.g., RabPON1) or Phe (*e.g.,* Human PON1, Mouse PON1 and Rat PON1; Fig. 8) in various wt PON1s that are known to exhibit almost identical enzymatic properties.

The third, and smallest, group includes three residues that were mutated during the shuffling and amplification processes and differ, therefore, from all four parental genes. These residues are all located on the protein surface (Fig. 9), and include positions 19, 123 and 260. Position 19 (Gly to Arg) varies between the different wt PON1s (Fig. 8) that are known to exhibit almost identical enzymatic properties. In addition, this position was mutated during the directed evolution of PON1 and selected (data not shown) without having any observable effect on the enzymatic activity. The mutation at position 123 (Glu to Asp) is subtle; this residue is located on the surface and, therefore, is highly unlikely to have any effect on enzymatic function. The third residue (260) was mutated from Lys to Arg. This is also a subtle mutation that, being on the surface, is unlikely to change the protein's properties.

In conclusion, it seems that none of the sequence variations seen between rePON1-G2E6 and wt rabbit PON1 are likely to affect its structure or function. PON1 appears to be insensitive to mutations at many positions, and can tolerate multiple amino acid substitutions at its surface and core, with no effect on its enzymatic function.

Methods

Expression and purification of native rePON1-G2E6 and its SeMet derivative

rePON1-G2E6 was expressed as a thioredoxin (Trx) fusion protein, with an incorporated HIS Tag, and purified by chromatography on a NiNTA column followed by High Trap Q column (Pharmacia) [10]. In the course of attempts to purify and crystallize it, we noticed that during storage the linker between the Trx and rePON1 was spontaneously cleaved, and that the crystals obtained contained only rePON1. The cause of this cleavage is still under investigation. It was observed in all rePON1 variants, and could even be mediated by PON1 itself. Subsequent crystallizations were set up with the cleaved and purified rePON1 as described below. Following purification of the Trx fusion product by capture on Ni-NTA beads followed by ion exchange chromatography[10], the protein was incubated at 25ºC for ten days. The cleavage was monitored by SDS-PAGE and mass spectrometry. The cleaved protein was concentrated and applied to HiLoad 26/60/ Superdex 200 (preparative grade, Pharmacia). Fractions from the main peak were analyzed again by SDS-PAGE, and by monitoring of enzymatic activity, pooled, and concentrated to 10mg/ml. Sodium azide was added to a concentration of 0.02%. Mass spectrometry indicated a mass of 40223±201Da. N-terminal Edman sequencing gave the following sequence: H_2N-DDDKAM. Both types of data are consistent with cleavage of the linker (expected mass spec 40108Da) 5 amino acid residues before the methionine residue that is PON1's first amino acid.

The SeMet-labeled rePON1-G2E6 was obtained as follows: a pET 32b plasmid coding for rePON1-G2E6[10] was freshly transformed into B834(DE3) cells, and plated on LB agar plates supplemented with Ampicillin. Colonies from three agar plates were scraped and rinsed (by resuspension and centrifugation) with M9 salt solution supplemented with 2mM $MgSO_4$, 0.4% Glucose, 25 μg/ml $FeSO_4$, 40 μg/ml of each of the 20 natural amino acids, with the exception of L-methionine, 40μg/ml of seleno-L-methionine, 1μg/ml of vitamins (Riboflavin, Niacinamide, Pyridoxine monohydrochloride and Thiamine) and 100µg/ml of Ampicillin. Typically, 1 L of M9 minimal media with the above supplements was inoculated with 5ml of rinsed *E. coli* colonies, and grown at 30ºC to OD_{600nm} = 0.7. Cultures were then transferred to 20ºC, and IPTG added to 0.5mM. Growth was continued for another 36 h at 20°C, after which the cells were

harvested, lysed and purified as above. Mass spectrometry indicated the incorporation of six SeMets per rePON1, including the Trx tag. Purification, cleavage from Trx, and isolation of rePON1 were performed as above.

Directed Evolution We used a recombinant PON1 gene variant (G3C9) cloned into a modified pET32b vector[10]. Librarieswere prepared by error-prone PCR amplifications of these genes, at biased dNTP concentrations, in the presence of manganese chloride, and by wobble-base PCR as previously described[10,14]. *E. coli* cells grown on agar plates were transformed with the resulting PON1 libraries. The plates were replicated, and screened for 2-naphtylacetate hydrolysis using Fast Red to detect the 2-naphthol product as previously described[10]. PON1 libraries were also screened with three additional substrates: 2-naphtyloctanoate was screened by Fast Red detection, and hydrolysis of the organophosphate substrate, 7-*O*-diethylphosphoryl-3-cyano-7-hydroxycoumarin, and the ester substrate, *O*-acetoxy-7-hydroxycoumarin, were screened by detecting the fluorescent coumarin products under a 360-nm ultraviolet lamp[14]. Positive clones identified from each screen were grown in liquid medium in individual wells of 96-well plates, lysed with BugBuster (Novagen), and assayed on a variety of substrates using a spectrophotometeric plate reader[10,14]. Plasmid DNA was extracted from all clones that had a significantly higher rate of hydrolysis relative to their respective starting gene (typically 3–10-fold higher) and subjected to DNA shuffling[20] to generate the second-generation libraries. Positive variants isolated from the second round of screening were reshuffled (PON1) to yield third-generation libraries that were screened with the same substrate.

The best PON1 variants from the last round of screening were overexpressed in Origami B (Novagen) *E. coli* cells and purified by affinity chromatography on Ni-NTA agarose (PON1 variants)[10]. Rates of product formation were assayed spectrophotometrically in 96-well plates using 200-μl reaction volumes as described[10,14]. Kinetic parameters were derived by fitting the initial rates of product release to the Michaelis-Menten model. Rates of hydrolysis for substrates with limited aqueous solubility had to be measured below the K_M concentrations, and k_{cat}/K_M values were derived directly ($k_{cat}/K_M = V_o/[E]_0[S]_0$).

Structure determination The structure was determined for rePON1 variant G2E6 (for its sequence see Fig. 6). The rePON1 variants were crystallized by the microbatch method under oil[36] using a Douglas Instruments IMPAX robot. Data were collected on beamline ID14-4 at the European Synchrotron Radiation Facility (Genoble, France), and processed with XDS[37]. Three datasets were collected for the SeMet protein at 100K, at Se peak wavelength (0.9794Å), in order to increase the redundancy and accuracy of the Se anomalous signal, while monitoring the extent of radiating damage. A data set for the native crystal was collected at a wavelength of 0.9796Å. Data collection statistics are given in Table 5.

Although PON1 bears no sequence similarity to any other protein sequence, it was suggested that it might have a 6-beta propeller conformation. As a consequence, solution of its structure was attempted by molecular replacement (MR), using the structure of 3-carboxy-*cis*, *cis*-muconate lactonizing enzyme (PDB-code 1jof) as a search template. A weak, but still significant, MR peak was found by the maximum likelihood program PHASER[38]. Although this did not result in structure solution, it did help in selecting the correct space group ($P4_32_12$). Three Se sites were located on the basis of the anomalous difference, using SHELXD after local scaling using XPREP[39]. SHELXE confirmed the correct space group and solvent content. Good experimental SIRAS (single isomorphous replacement anomalous scattering) phases were obtained using the program SHARP[40], while refining 3 Se sites against the 2.2Å native and 2.6Å Se SAD data, resulting in an overall figure of merit (FOM) of 0.11/0.06 for the acentric/centric reflections, respectively. The isomorphous difference phasing power was very low (0.22 overall) due to the lack of isomorphism between the native and SeMet data sets. However, the anomalous phasing power for the SeMet SAD data set was good to at least 4Å (0.74 overall). Phases were improved by applying solvent flipping density modification using SOLOMON[41], as directed by SHARP, using a 63% solvent content, yielding an overall FOM of 0.88. An automated tracing program ARP/wARP[42], using native amplitudes to 2.2Å, coupled with experimental phase restraints, resulted in an automatic tracing of *ca.* 95% of the chain. Manual model completion was performed using program O[43], iterated with refinement using REFMAC[44]. The refinement and model statistics are listed in Table 5.

Figures were created with PyMol (http://pymol.sourceforge.net/) and MolScript (Fig. 5; http://www.avatar.se/molscript). Accessible surface area was calculated by the program AREAIMOL in the CCP4 package[45]. Coordinates were deposited in the PDB, entry 1v04.

Directed evolution rePON1 variant G3C9 was used as the starting point for directed evolution. It exhibits a sequence almost identical to those of wt rabbit PON1 and rePON1 variant G2E6, whose 3D-structure was determined (91% identity), and the same enzymatic parameters. Libraries were generated and cloned as described[10]. PTE activity was screened, and subsequently quantified, with the fluorogenic OP substrate, 7-*O*-diethylphosphoryl-3-cyano-7-hydroxycoumarin, as described[10]. Thiolactonase activity was initially screened for with 2NA on agar plates. Positive clones were picked from replica plates and grown in 96-well plates as described[10]. The crude cell lysates and purified proteins were assayed for hydrolysis of γ-butyrothiolactone using 5,5'-dithio-bis-2-nitrobenzoic acid for detection of product by absorbance at 412 nm. Esterase activity was screened with the fluorogenic substrate, 7-acetoxycoumarin (for short-chain esterase activity), or with 2-naphthyl octanoate (for long-chain esterase activity) using Fast Red for detection of 2-naphthol[10]. Colonies exhibiting the highest activity were grown in 96-well plates, and the crude cell lysates were assayed spectrophotometrically at 365 nm, for hydrolysis of 7-acetoxycoumarin, and at 320 nm with 2-naphthyl laurate. The activity of the variants described above was determined with the same substrates and assays.

Enzyme kinetics k_{cat} and K_M values were determined for rePON1-G2E6 with 2NA and paraoxon[10], at pH 5.6-9.5. Buffers used were MES (pH 5.6–6.5) and bis-tris propane (pH 6.5–9.4) at 0.1M, plus 1mM $CaCl_2$; the ionic strength was adjusted to 0.2M with NaCl. Kinetic parameters were obtained from 3–5 independent measurements averaged with standard deviations of 2–23%.

Tables

Table 1. New PON1 variants generated by directed evolution

Variant		Phospho-triesterase activity[a]	Lactonase activity[a]	Esterase activity[a]	
				***short chain* ester**	***long chain* esters**
rePON1 (wt-like activity)		$3.5*10^3$	$1.4*10^2$	$3.0*10^4$	$1.7*10^2$
DIRECTLY-EVOLVED VARIANTS WITH 'SPECIALIZED' SUBSTRATE SELECTIVITIES					
#	**Mutations**[b]				
7PC	**V346A**	$1.3*10^4$ **(3.7)**[b]	$5.0*10^1$ (0.36)	$1.4*10^3$ (0.05)	$1.4*10^1$ (0.08)
4PC	**L69V**, **S193P**, **V346A**	$5.7*10^4$ **(16.3)**	0.9 (0.006)	$4.4*10^2$ (0.015)	n.d
1HT	**I291L**, **T332A**, G339E	$6.0*10^2$ (0.17)	$3.0*10^3$ **(25.9)**	$8.6*10^3$ (0.3)	n.d.
2AC	**F292S**, **V346M** V30A, E249K	$1.1*10^2$ (0.03)	6.4 (0.04)	$6.0*10^5$ **(20)**	$7.0*10^2$ (4.1)
7HY	**F292V**, **Y293D**, I109M	$4.1*10^1$ (0.01)	4.1 (0.03)	$1.2*10^5$ (4.0)	$8.0*10^3$ (**47**)
4HY	**I74L**, **F292L** K84Q, I343M	$5.3*10^1$ (0.015)	5.9 (0.04)	$5.2*10^4$ (1.7)	$6.5*10^3$ **(38)**

[a] Activities are expressed as μmoles of product released per minute per mg enzyme. In parentheses are the activities of the new variants relative to wt PON1's activity on the same substrate.

[b] Mutations are given in relation to the sequence of the wt-like variant G3C9. In bold are positions found to be mutated in all the highest-activity variants for a given substrate. Typically, the same mutations could be individually identified in the sequence of selected variants from the 1st and 2nd rounds of evolution, and appear together in the 3rd generation variants. Mutations that appear in only one selected variant, but not in others selected for the same substrate, and/or do not appear in the 1st and 2nd round of evolution, are noted in regular print.

Table 2 New PON1 variants generated by site-directed mutagenesis

Mutation	Aryl-esterase (% relative to wt)	Paraoxonase (% relative to wt)
His115Gln	0.6%	32%
His115Trp	0.056%	195%
His134Gln	9.9%	600%

Table 3. Selectivity-determining residues of PONs

Sub-family	PON1	PON2	PON3	Newly-evolved PON1s	
Position				Residue	Selectivity
69	L	L	L	V/I	PTE[a]
74[b]	I	L	M	L/M	lactonase/esterase
75[b]	K/M	K/H	P		
76[b]	S	S	N/A		
78[b]	N/D	A	A		
190	Y	F/I	L/V/F		
192	K/R	K/M	S/A/V		human R/Q SNP
193	S	Y/F	F/L	P	PTE[a]
196	M	M/T	M		
222	F	S	S		
240	L	I	V		
291	I	L/V	L	L	lactonase
292	F	F/Y	L	L/V/S	esterase
293	F/Y	V/Y/I	N/I	D	lipase-like[c]
332	T	S	S/T	A	lactonase
346	V	L/V	I/V	A	PTE[a]

[a] PTE = phosphotriesterase. It should be noted that the PTE activity of these mutants is much higher than that of wt PON1, which is the best PTE of the three PONs (Table 1).

[b] Residues 74–79 belong to the selectivity-determining residues which differ between the PON subfamilies (Fig. 6), but are conserved within them. These residues are part of a mobile loop (72–79) containing residue 74, which is not seen in the electron density but is presumably part of the active site.

[c] Lipase-like activity refers to esters of long-chain carboxylic acids (Table 1).

Table 4. Amino acid changes in G2E6 relative to Rabbit PON1

Group	Mutations[a]	Origin	Location and nature[c]
I	T126, L130, S138, V143, G301, V320, L341, I343	wild type Human, Mouse, Rat, PON1	hydrophobic core; conserved residues among all soluble PON variants.
II	M12, K93, E94, A96, S98, E101, I103, N105, L107, I109, I121, E149, V261, S263, D265, F293, A296, E297, E313, D354.	wild type Human, Mouse, Rat, PON1	protein surface; non-conserved between different soluble PON1 variants.
III	R19, D123,R260	Mutation[b]	protein surface

[a] The rePON1-G2E6 sequence was aligned to the rabbit PON1 protein sequence using ClustaWI. Amino acid identities are to the rePON1-G2E6 sequence.

[b] Mutations that occurred during the shuffling process into an amino acid that is different relative to all four wt PON1 genes.

[c] The precise locations of these amino acids on PON1's structure are shown in Fig. 9.

Table 5 Data collection and refinement statistics.

Data collection

	Native	SeMet protein
Wavelength (Å)	0.9796	0.9794
Unit cell (Å)	98.44, 139.17	98.49, 139.56
Space group	$P4_32_12$	$P4_32_12$
Resolution range (Å)	20–2.2	30–2.6
Number of unique reflections	35,312	39,473
Completeness (%)[a]	99.7 (97.9)	97.8 (97.7)
$I/\sigma(I)$[a]	12.7 (2.7)	13.7 (4.2)
$R_{sym}(I)$ (%)[a]	8.6 (66.1)	10.4 (51.0)

Refinement and model statistics

Resolution range (Å)	20–2.2
Number of reflections	33,505
R-factor: work, free (%)	18.5, 21.7
Average B-factors ($Å^2$)	34.76
RMSD from ideal values:	
Bond length (Å)	0.028
Bond angle (^{o})	2.02
Dihedral angles (^{o})	28.7
Improper torsion angles (^{o})	2.06
Estimated coordinate error:	
Low resolution cutoff (Å)	5.0
ESD from Luzzati plot (Å)	0.32
ESD from SIGMAA (Å)	0.34
Ramachandran outliers (%)[b]	3.9

[a] Data for the outer shell given in parentheses.

[b] Ramachandran plot outliers are all glycines except for H115, N224, D269 and H348.

Figures

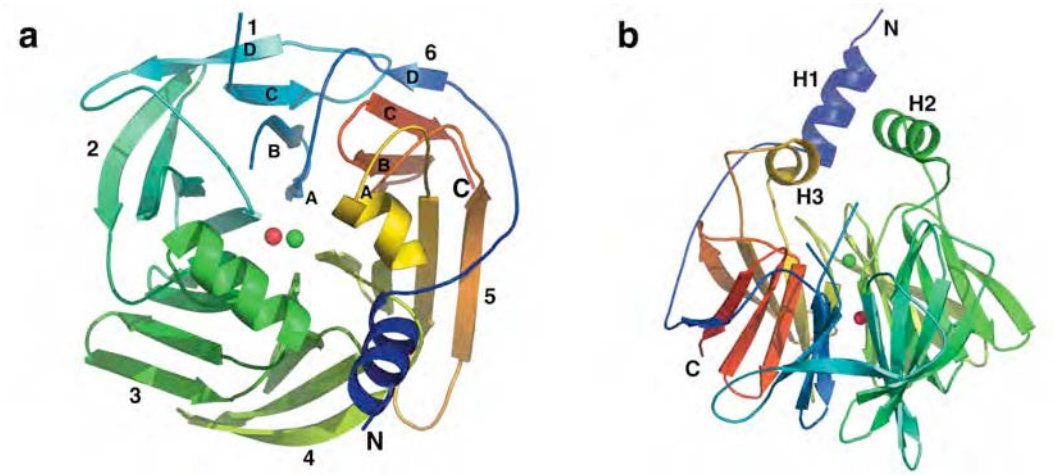

Fig. 1. Overall structure of PON1. (**a**) A view of the 6-bladed β-propeller from its top. The top of the propeller is, by convention, the face carrying the loops connecting the outer β-strand of each blade (strand D) with the inner strand (A) of the next blade[17]. Shown are the N- and C-termini, and the two calcium atoms in the central tunnel of the propeller (Ca-1 in green, Ca-2 in red). (**b**) A side view of the propeller, including the three helices at the top of the propeller (H1–H3). N-terminal residues 1–15, and a surface loop connecting strands 1B and 1C (residues 72–79), are not seen in the structure.

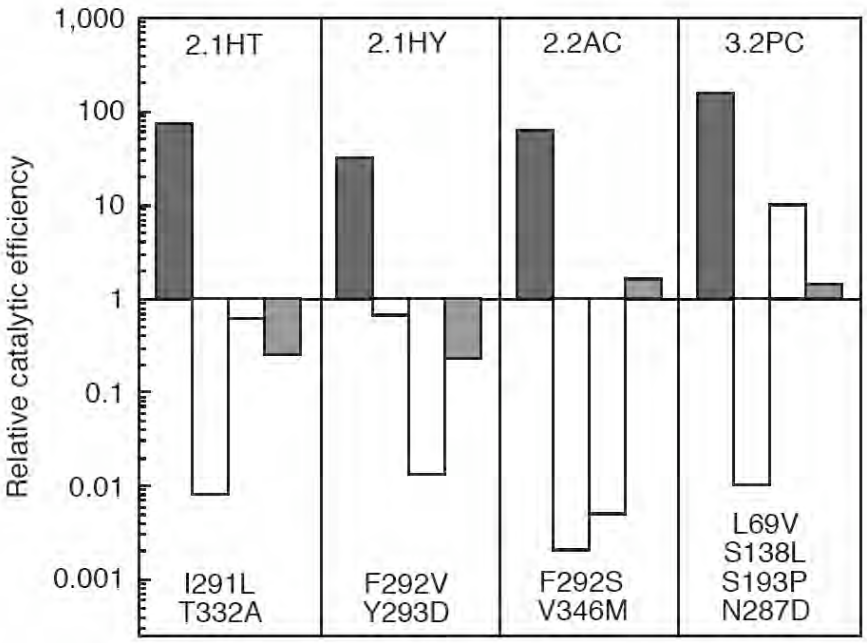

Fig. 2. Changes in activities of the newly evolved PON1 variants. The ratios of k_{cat}/K_M values relative to wild-type PON1 for four evolved variants and the mutations observed in them are plotted. Black bars, the promiscuous substrate for which each variant was evolved (2.1HT was evolved for γ-butyryl thiolactone, 2.1HY for 2-naphtyl octanoate, 2.2AC for *O*-acetoxy-7-hydroxycoumarin, and 3.2PC for the organophosphate 7-*O*-diethylphosphoryl-3-cyano-7-hydroxycoumarin); white bars, two other promiscuous substrates (phenyl acetate, left; paraoxon, right); gray bars, dihydrocoumarin, representing the native lactonase activity of PON1.

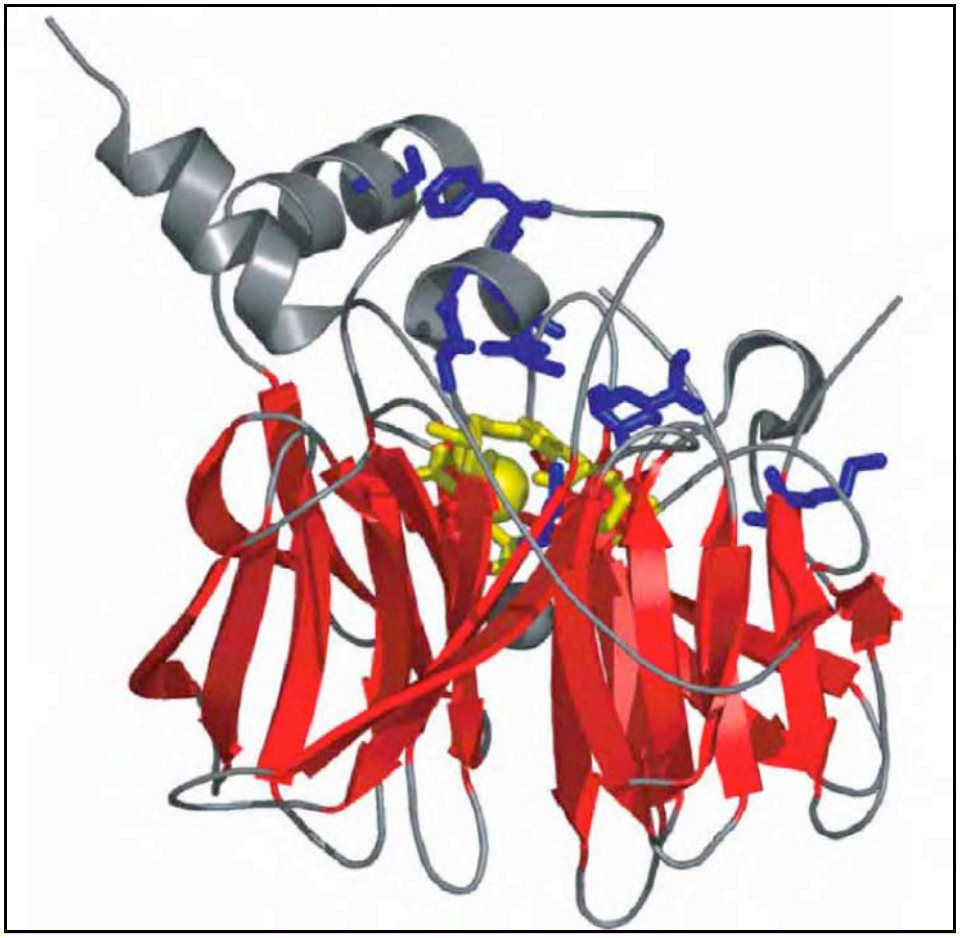

Fig. 3. The location of the selectivity-changing mutations observed in the directly evolved PON1 variants. The six-bladed β-propeller scaffold is shown in red, with the structural calcium in its central tunnel shown in gray; the catalytic machinery (the top calcium atom and its ligating residues, and His115) are shown in yellow. The residues that give rise to marked changes in the promiscuous activities of directly evolved PON1, but barely change its native lactonase activity (Fig. 1), are shown in blue. They are not part of the scaffold of PON1 or of the catalytic machinery that is linked to this scaffold. Rather, the selectivity-changing residues are on surface loops, and helices connected to these loops, that 'decorate' the scaffold and form the substrate-binding pocket. These loops tend to have great conformational flexibility. Some of the mutations observed in PON1 are in a loop that is disordered and not visible in the crystal structure (residues 72–79)[27]. The PON1 structure (PDB entry 1V04)[27] was drawn with PyMol[46].

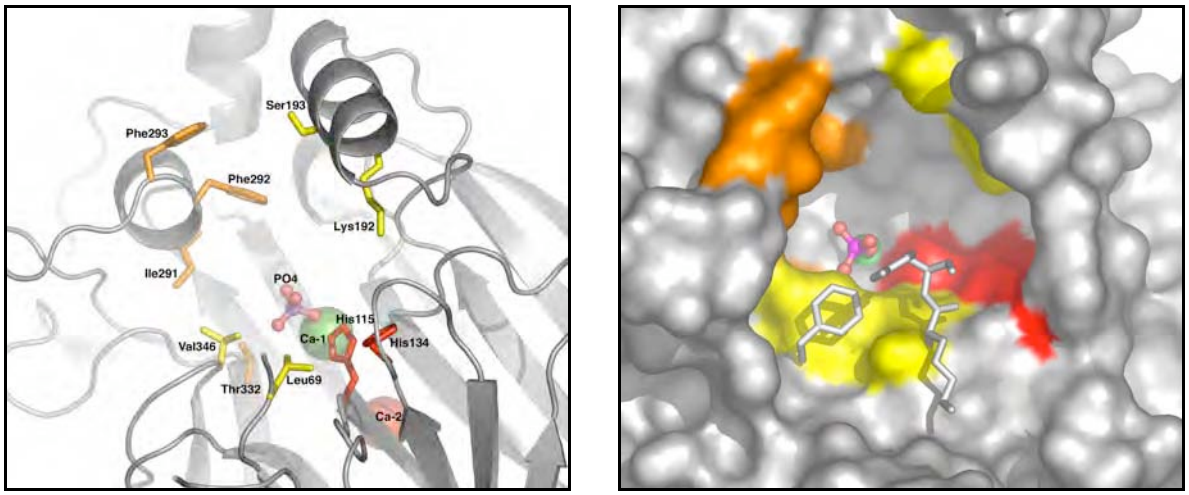

(a) (b)

Fig. 4. The active site of PON1 viewed from above the propeller. (**a**) Shown are the central tunnel of the propeller with the two calcium atoms, and the side-chains of the residues found to be mutated in the newly-evolved PON1 variants for esterase and lactonase (in orange) or for PTE activity (in yellow), including position 192 of the Q/R (Gln/Arg) human polymorphism. Shown in red is the putative catalytic His-dyad (see *The catalytic mechanism* section and **Fig. 3**). (**b**) A surface view of the active site. Lys70, Tyr71and Phe347 are shown as sticks, to permit a better view of the active site. At the deepest point of the cavity lies the upper calcium atom (Ca-1 in green) to which a phosphate ion (PO_4) is bound.

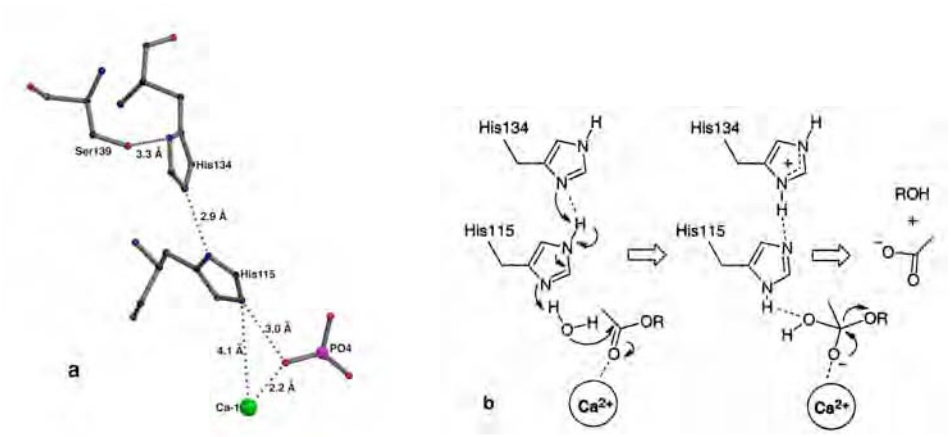

Fig 5. The postulated catalytic site and mechanism of PON1. (**a**) The catalytic site: the upper calcium atom (Ca-1), the phosphate ion found at the bottom of the active site, and the postulated His-dyad. (**b**) A schematic representation of the proposed mechanism of action of PON1 on ester substrates such as phenyl and 2-naphthylacetate. The first step involves deprotonation of a water molecule by the His-dyad to generate an hydroxide anion which attacks the ester carbonyl, producing an oxyanionic, tetrahedral intermediate. This intermediate breaks down (second step) to an acetate ion and either phenol or 2-naphthol.

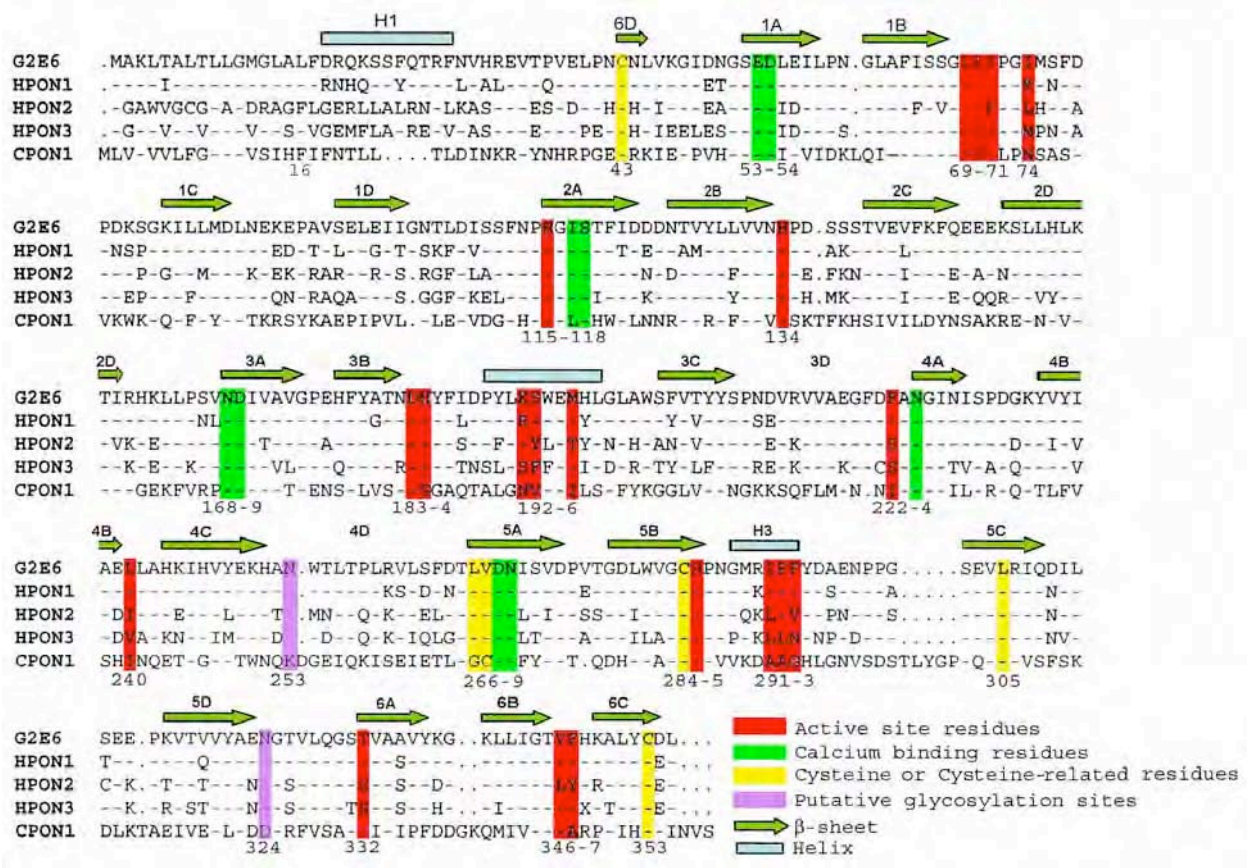

Fig 6. Sequence alignment of representative members of the PON family. Shown are human PON1, PON2 and PON3 (with an 'H' prefix), *C. elegans* PON1 (CPON1), and rePON1 variant G2E6, the structure of which is reported here.

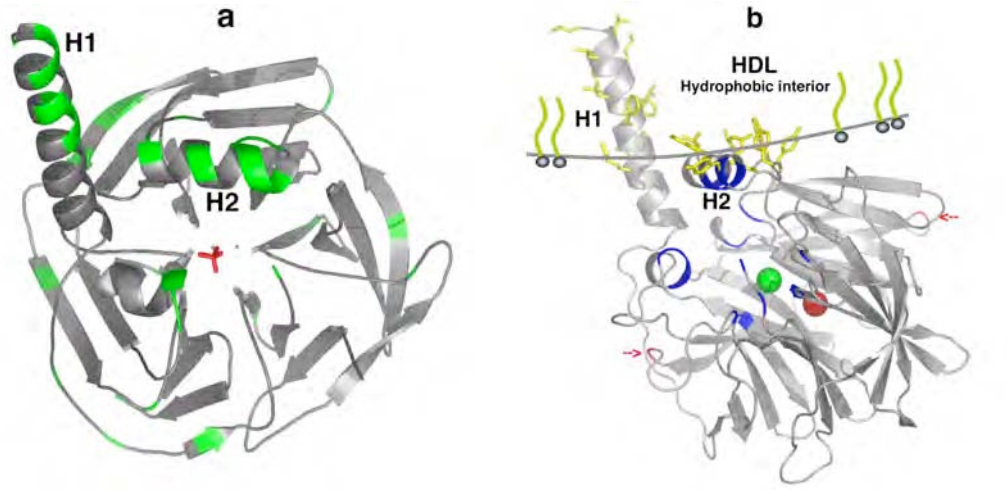

Fig 7. The proposed model for anchoring of PON1 to the surface of HDL. (**a**) Tertiary structure cartoon of rePON1 showing its exposed hydrophobic surfaces. N-terminal residues 7–18, missing in the crystal structure, and predicted to be helical, were modeled as part of H1. Denoted are *all* the hydrophobic residues (L,F,P,I,Y,W,V) appearing with accessible surface area ≥20Å^2. (**b**) Hydrophobic residues proposed to be involved in HDL-anchoring are shown with their side-chains in yellow. The line - defined by the side chains of Tyr185, Phe 186, Tyr190, Trp194, Trp202 (helix H2 and the adjacent loops) and Lys21 (helix H1) - models the putative interface between HDL's hydrophobic interior and the exterior aqueous phase. The active site and the selectivity-determining residues (Table 2) are marked in blue, and the proposed glycosylation sites (Asn253 and Asn324) in red.[13,18]

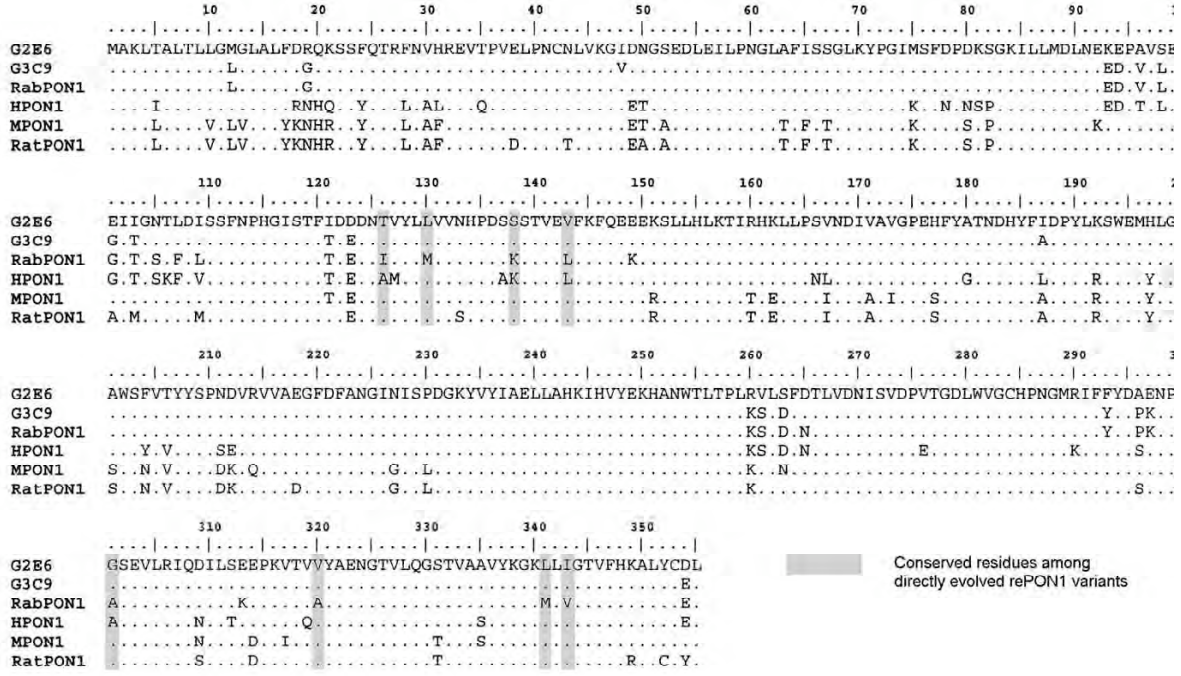

Fig 8. Multiple sequence alignment of human (H), rat, mouse (M) and rabbit (Rab) PON1, and rePON1 variants G2E6 and G3C9.

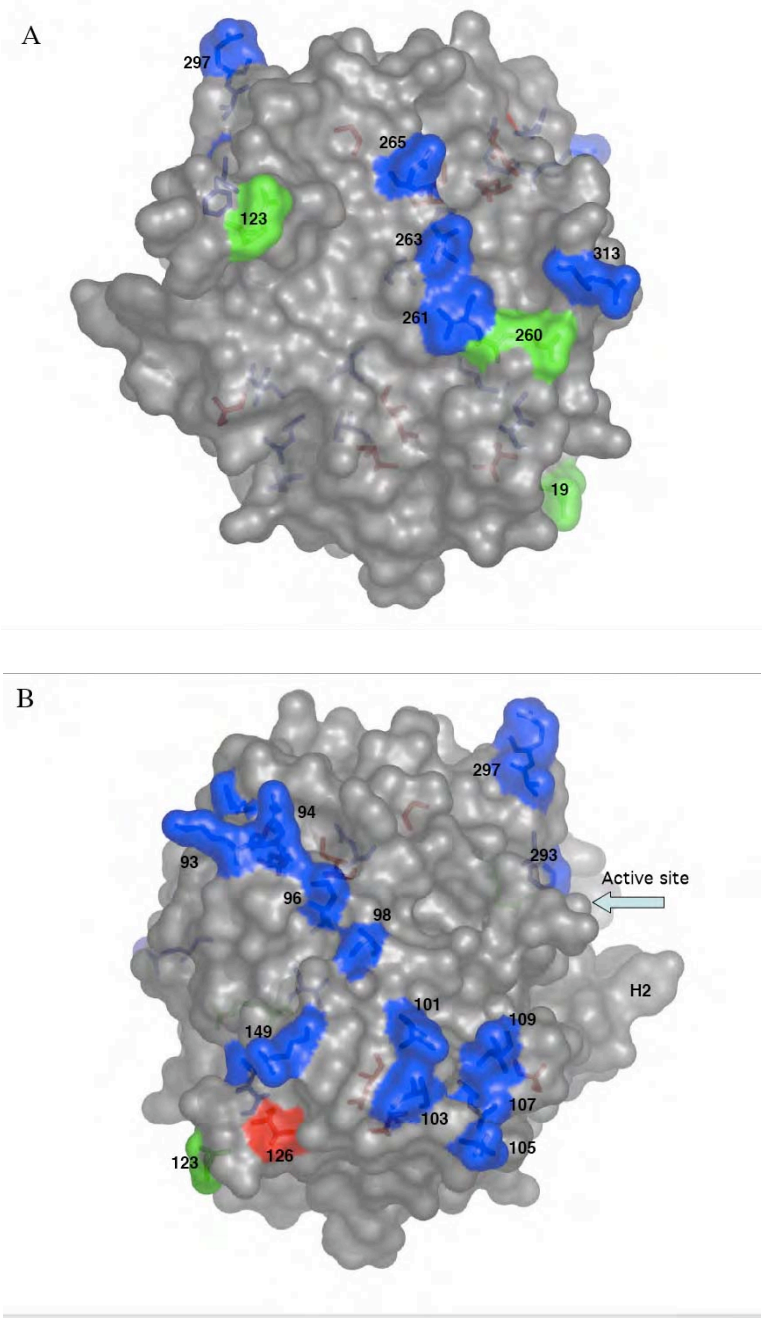

Fig 9. Two surface representations taken from the side of the β-propeller – one rotated 180° relative to the other. The amino acid variations between rePON1 variant G2E6 and wt RabPON1 are marked: In red are amino acids that originate from human, mouse and rat PON1, and are conserved among all the rePON1 variants expressed in *E. coli* (Table 1, group I). In blue - amino acids that originate from human, mouse and rat PON1 that are *not* conserved among soluble rePON1 variants (Table 1, group II). In green - amino acids that were mutated during the DNA shuffling process (Table 4, group III). The figure was created by PyMol (http://pymol.sourceforge.net/).

Key Research Accomplishments

- 6 new PON1 variants were generated by directed evolution:
    - 7PC – V346A
    - 4PC – L69V, S193P, V346A
    - 1HT – I291L, T332A, G339E]
    - 2AC – F292S, V346M, V30A, E249K
    - 7HY – F292V, Y293D, I109M,
    - 4HY – I74L, F292L, K84Q, I343M
- These new PON1 variants displayed a repertoire of specificities towards ester and organophosphate substrates, thus demonstrating the potential to engineer variants with beneficial scavenger activities.
- Crystals of RePON1-G2E6 (which exhibit 91% identity to wt rabbit PON1) were obtained, as were as well homologous crystals of the Se-Met derivative.
- X-ray data sets were collected to for the native crystals to 2.2Å and for the Se-Met derivative to 2.6Å resolution.
- The X-ray data sets were used to determine, for the first time, the 3D crystal structure of paraoxonase.
- The 3D structure permitted identification of the active site and led to a proposed catalytic mechanism of paraoxonase

Reportable Outcomes

Manuscripts:

1. Aharoni, A., Gaidukov, L., Yagur, S., Toker, L., Silman, I. & Tawfik, D.S. (2004). "Directed evolution of mammalian paraoxonases PON1 and PON3 for bacterial expression and catalytic specialization" *Proc. Natl. Acad. Sci. USA* **101**, 482-487.

2. Harel, M., Aharoni, A., Gaidukov, L., Brumshtein, B., Khersonsky, O., Meged, R., Dvir, H., Ravelli, R.B., McCarthy, A., Toker, L., Silman, I., Sussman, J.L. & Tawfik, D.S. (2004). "Structure and evolution of the serum paraoxonase family of detoxifying and anti-atherosclerotic enzymes" *Nat. Struct. Mol. Biol.* **11**, 412-419.

3. Harel, M., Aharoni, A., Gaidukov, L., Brumshtein, B., Khersonsky, O., Meged, R., Dvir, H., Ravelli, R.B., McCarthy, A., Toker, L., Silman, I., Sussman, J.L. & Tawfik, D.S. (2004). "Corrigendum: Structure and evolution of the serum paraoxonase family of detoxifying and anti-atherosclerotic enzymes" *Nat. Struct. Mol. Biol.* **11**, 1253.

Abstracts:

1. Aharoni, A. (2004) "Directed Evolution of Paraoxonases PON1 and PON3 for Bacterial Expression and Catalytic Specialization" First International Conference on "Paraoxonases - Basic and Clinical Directions of Current Research" 22-24 April 2004, Michigan Union, University of Michigan, Ann Arbor, USA.

2. Sussman, J.L. (2004) "The 3D-Structure, Mechanism and Evolution of Serum Paraoxonases" 22-24 April 2004, Michigan Union, University of Michigan, Ann Arbor, USA.

3. Sussman, J.L, Aharoni, A., Harel, M., Gaydukov, L., Brumshtein, B., Meged, R., Khersonsky, O., Toker, L., Silman, I. & Tawfik, D.S. (2004) "3D Structure of Mammalian Paraoxonase at 2.2Å Resolution" 2004 Medical Defense Bioscience Review, 16-21 May 2004, Hunt Valley, MD, USA.

4. Sussman, J.L., Silman, I., Harel, M., Aharoni, A., Gaidukov, L, Brumshtein, B. Khersonsky, O., Toker, L., & Tawfik, D.S. (2004) "The 3D-Structure, Mechanism and Evolution of Serum Paraoxonases" DECON 2004, 16-20 May 2004, Palm Harbor, FL, USA

5. Sussman, J.L. (2004) “3D-Structure, Mechanism and Evolution of Serum Paraoxonases – a Family of Detoxifying and Anti-Atherosclerotic Enzymes” Life Science Seminar, 15-June-2004, Brookhaven National Laboratory, Upton, NY, USA

Conclusions

Directed molecular evolution, which involved shuffling of the PON1 genes of four mammalian species, was used to produce soluble and catalytically active paraoxonase in *E. coli* in milligram quantities. A number of different mutants were produced which differed in their specificity towards ester and organophosphate substrates. These findings demonstrate the potential of molecular evolution to generate PON1 variants tailor made for serving as nerve agent scavengers.

One new variant was crystallized and its crystal structure subsequently determined. The 3D structure was revealed to be a 6-blade β-propeller. The active was found to be within the central cavity of the propeller and a plausible reaction mechanism was suggested.

References

1. Draganov, D.I. & La Du, B.N. Pharmacogenetics of paraoxonases: a brief review. *Naunyn Schmiedebergs Arch. Pharmacol.* **369**, 78-88 (2004).
2. Lusis, A.J. Atherosclerosis. *Nature* **407**, 233-241 (2000).
3. Shih, D.M., Gu, L., Xia, Y.R., Navab, M., Li, W.F., Hama, S., Castellani, L.W., Furlong, C.E., Costa, L.G., Fogelman, A.M. & Lusis, A.J. Mice lacking serum paraoxonase are susceptible to organophosphate toxicity and atherosclerosis. *Nature* **394**, 284-287 (1998).
4. Mackness, M.I., Arrol, S. & Durrington, P.N. Paraoxonase prevents accumulation of lipoperoxides in low-density lipoprotein. *FEBS Lett.* **286**, 152-154 (1991).
5. Reddy, S.T., Wadleigh, D.J., Grijalva, V., Ng, C., Hama, S., Gangopadhyay, A., Shih, D.M., Lusis, A.J., Navab, M. & Fogelman, A.M. Human paraoxonase-3 is an HDL-associated enzyme with biological activity similar to paraoxonase-1 protein but is not regulated by oxidized lipids. *Arterioscler. Thromb. Vasc. Biol.* **21**, 542-547 (2001).
6. Rodrigo, L., Mackness, B., Durrington, P.N., Hernandez, A. & Mackness, M.I. Hydrolysis of platelet-activating factor by human serum paraoxonase. *Biochem. J.* **354**, 1-7 (2001).
7. Ahmed, Z., Ravandi, A., Maguire, G.F., Emili, A., Draganov, D., La Du, B.N., Kuksis, A. & Connelly, P.W. Apolipoprotein A-I promotes the formation of phosphatidylcholine core aldehydes that are hydrolyzed by paraoxonase (PON-1) during high density lipoprotein oxidation with a peroxynitrite donor. *J. Biol. Chem.* **276**, 24473-24481 (2001).
8. Jakubowski, H. Calcium-dependent human serum homocysteine thiolactone hydrolase. A protective mechanism against protein N-homocysteinylation. *J. Biol. Chem.* **275**, 3957-3962 (2000).
9. Sorenson, R.C., Bisgaier, C.L., Aviram, M., Hsu, C., Billecke, S. & La Du, B.N. Human serum Paraoxonase/Arylesterase's retained hydrophobic N-terminal leader sequence associates with HDLs by binding phospholipids: apolipoprotein A-I stabilizes activity. *Arterioscler. Thromb. Vasc. Biol.* **19**, 2214-2225 (1999).
10. Aharoni, A., Gaidukov, L., Yagur, S., Toker, L., Silman, I. & Tawfik, D.S. Directed evolution of mammalian paraoxonases PON1 and PON3 for bacterial expression and catalytic specialization. *Proc. Natl. Acad. Sci. USA* **101**, 482-487 (2004).
11. Fokine, A., Morales, R., Contreras-Martel, C., Carpentier, P., Renault, F., Rochu, D. & Chabriere, E. Direct phasing at low resolution of a protein copurified with human paraoxonase (PON1). *Acta Crystallographica D Biological Crystallograrphy* **59**, 2083-2087 (2003).
12. Josse, D., Ebel, C., Stroebel, D., Fontaine, A., Borges, F., Echalier, A., Baud, D., Renault, F., Le Maire, M., Chabrieres, E. & Masson, P. Oligomeric states of the detergent-solubilized human serum paraoxonase (PON1). *J. Biol. Chem.* **277**, 33386-33397 (2002).
13. Kuo, C.L. & La Du, B.N. Comparison of purified human and rabbit serum paraoxonases. *Drug Metab. Dispos.* **23**, 935-944 (1995).
14. Harel, M., Aharoni, A., Gaidukov, L., Brumshtein, B., Khersonsky, O., Meged, R., Dvir, H., Ravelli, R.B., McCarthy, A., Toker, L., Silman, I., Sussman, J.L. & Tawfik, D.S. Structure and evolution of the serum paraoxonase family of detoxifying and anti-atherosclerotic enzymes. *Nat. Struct. Mol. Biol.* **11**, 412-419 (2004).

15. Jawad, Z. & Paoli, M. Novel sequences propel familiar folds. *Structure (Camb)* **10**, 447-454 (2002).

16. Kuo, C.L. & La Du, B.N. Calcium binding by human and rabbit serum paraoxonases. Structural stability and enzymatic activity. *Drug Metab. Dispos.* **26**, 653-660 (1998).

17. Scharff, E.I., Koepke, J., Fritzsch, G., Lucke, C. & Ruterjans, H. Crystal structure of diisopropylfluorophosphatase from Loligo vulgaris. *Structure (Camb)* **9**, 493-502 (2001).

18. Josse, D., Xie, W., Renault, F., Rochu, D., Schopfer, L.M., Masson, P. & Lockridge, O. Identification of residues essential for human paraoxonase (PON1) arylesterase/organophosphatase activities. *Biochemistry* **38**, 2816-2825 (1999).

19. Arnold, F.H., Wintrode, P.L., Miyazaki, K. & Gershenson, A. How enzymes adapt: lessons from directed evolution. *TIBS* **26**, 100-106 (2001).

20. Stemmer, W.P. DNA shuffling by random fragmentation and reassembly: in vitro recombination for molecular evolution. *Proc. Natl. Acad. Sci. USA* **91**, 10747-10751 (1994).

21. Bone, R., Silen, J.L. & Agard, D.A. Structural plasticity broadens the specificity of an engineered protease. *Nature* **339**, 191-195 (1989).

22. Perona, J.J. & Craik, C.S. Evolutionary divergence of substrate specificity within the chymotrypsin-like serine protease fold. *J. Biol. Chem.* **272**, 29987-29990 (1997).

23. James, L.C. & Tawfik, D.S. The specificity of cross-reactivity: promiscuous antibody binding involves specific hydrogen bonds rather than nonspecific hydrophobic stickiness. *Protein Sci.* **12**, 2183-2193 (2003).

24. Sekar, K., Yu, B.Z., Rogers, J., Lutton, J., Liu, X., Chen, X., Tsai, M.D., Jain, M.K. & Sundaralingam, M. Phospholipase A2 engineering. Structural and functional roles of the highly conserved active site residue aspartate-99. *Biochemistry* **36**, 3104-3114 (1997).

25. Josse, D., Xie, W., Masson, P., Schopfer, L.M. & Lockridge, O. Tryptophan residue(s) as major components of the human serum paraoxonase active site. *Chem. Biol. Interactions* **119-120**, 79-84 (1999).

26. Yeung, D.T., Josse, D., Nicholson, J.D., Khanal, A., McAndrew, C.W., Bahnson, B.J., Lenz, D.E. & Cerasoli, D.M. Structure/function analyses of human serum paraoxonase (HuPON1) mutants designed from a DFPase-like homology model. *Biochim. Biophys. Acta* **1702**, 67-77 (2004).

27. Harel, M., Aharoni, A., Gaidukov, L., Brumshtein, B., Khersonsky, O., Meged, R., Dvir, H., Ravelli, R.B., McCarthy, A., Toker, L., Silman, I., Sussman, J.L. & Tawfik, D.S. Corrigendum: Structure and evolution of the serum paraoxonase family of detoxifying and anti-atherosclerotic enzymes. *Nat. Struct. Mol. Biol.* **11**, 1253 (2004).

28. Aviram, M., Billecke, S., Sorenson, R., Bisgaier, C., Newton, R., Rosenblat, M., Erogul, J., Hsu, C., Dunlop, C. & La Du, B. Paraoxonase active site required for protection against LDL oxidation involves its free sulfhydryl group and is different from that required for its arylesterase/paraoxonase activities: selective action of human paraoxonase allozymes Q and R. *Arterioscler. Thromb. Vasc. Biol.* **18**, 1617-1624 (1998).

29. Borhani, D.W., Rogers, D.P., Engler, J.A. & Brouillette, C.G. Crystal structure of truncated human apolipoprotein A-I suggests a lipid-bound conformation. *Proc. Natl. Acad. Sci. USA* **94**, 12291-12296 (1997).

30. Segrest, J.P., Harvey, S.C. & Zannis, V. Detailed molecular model of apolipoprotein A-I on the surface of high-density lipoproteins and its functional implications. *Trends Cardiovasc. Med.* **10**, 246-252 (2000).
31. Killian, J.A. & von Heijne, G. How proteins adapt to a membrane-water interface. *TIBS* **25**, 429-434 (2000).
32. Bencharit, S., Morton, C.L., Xue, Y., Potter, P.M. & Redinbo, M.R. Structural basis of heroin and cocaine metabolism by a promiscuous human drug-processing enzyme. *Nat. Struct. Biol.* **10**, 349-356 (2003).
33. Millard, C.B., Lockridge, O. & Broomfield, C.A. Organophosphorus acid anhydride hydrolase activity in human butyrylcholinesterase: synergy results in a somanase. *Biochemistry* **37**, 237-247 (1998).
34. Greenblatt, H.M., Dvir, H., Silman, I. & Sussman, J.L. Acetylcholinesterase: a multifaceted target for structure-based drug design of anticholinesterase agents for the treatment of Alzheimer's disease. *J. Mol. Neurosci.* **20**, 369-384 (2003).
35. Leviev, I., Deakin, S. & James, R.W. Decreased stability of the M54 isoform of paraoxonase as a contributory factor to variations in human serum paraoxonase concentrations. *J. Lipid Res.* **42**, 528-535 (2001).
36. Chayen, N.E., Stewart, P.D.S., Maeder, D.L. & Blow, D.M. An Automated System for Micro-Batch Protein Crystallization and Screening. *J. Appl. Cryst.* **23**, 297-302 (1990).
37. Kabsch, W. Automatic processing of rotation diffraction data from crystals of initially unknown symmetry and cell constants. *J. Appl. Cryst.* **26**, 795-800 (1993).
38. Storoni, L.C., McCoy, A.J. & Read, R.J. Likelihood-enhanced fast rotation functions. *Acta Crystallographica D Biological Crystallogrrarphy* **60**, 432-438 (2004).
39. Uson, I. & Sheldrick, G.M. Advances in direct methods for protein crystallography. *Curr. Opin. Struct. Biol.* **9**, 643-648 (1999).
40. de La Fortelle, E. & Bricogne, G. "MaximumLikelihood Heavy-Atom Parameter Refinement in the MIR and MAD Methods". in *Methods Enzymol.*, Vol. 276 (eds. Carter, C.W. & Sweet, R.M.) 472-494 (Academic Press, 1996).
41. Abrahams, J.P. & Leslie, A.G. Methods used in the structure determination of bovine mitochondrial F1 ATPase. *Acta Crystallographica D Biological Crystallogrrarphy* **52**, 30-42 (1996).
42. Perrakis, A., Morris, R. & Lamzin, V.S. Automated protein model building combined with iterative structure refinement. *Nat. Struct. Biol.* **6**, 458-463 (1999).
43. Jones, T.A., Zou, J.-Y., Cowan, S.W. & Kjeldgaard, M. Improved methods for building protein models in electron density maps and the location of errors in these models. *Acta Cryst.* **A47**, 110-119 (1991).
44. Murshudov, G.N., Vagin, A.A., Lebedev, A., Wilson, K.S. & Dodson, E.J. Efficient anisotropic refinement of macromolecular structures using FFT. *Acta Crystallographica D Biological Crystallogrrarphy* **55 (Pt 1)**, 247-255 (1999).
45. Lee, B.K. & Richards, F.M. The Interpretation of Protein Structures Estimation of Static Accessibility. *J. Mol. Biol.* **55**, 379-400 (1971).
46. DeLano, W.L. The PyMOL Molecular Graphics System. (2002).

Appendices

none